

# UTILIZING CYLINDER PRESSURE DATA FOR COMPRESSION RATIO ESTIMATION

Marcus Klein \* Lars Eriksson \*

\* Linköpings Universitet, SE-581 83 Linköping, SWEDEN.

Abstract: Four methods for compression ratio estimation based on cylinder pressure traces are developed and evaluated for simulated and experimental cycles. Three methods rely upon a model of polytropic compression for the cylinder pressure. It is shown that they give good estimates with a small bias at low compression ratios. A variable projection algorithm with a logarithmic norm of the cylinder pressure yields the smallest confidence intervals and shortest computational time for these three methods. This method is recommended when computational time is an important issue. The polytropic pressure model lacks information about heat transfer and therefore the estimation bias increases with compression ratio. The fourth method includes heat transfer, crevice effects, and a commonly used heat release model for firing cycles. This method estimates the compression ratio more accurately in terms of bias and variance. The method is more computationally demanding and thus recommended when estimation accuracy is the most important property. In order to estimate the compression ratio as accurately as possible, motored cycles with high initial pressure should be used. *Copyright ©2005 IFAC*

Keywords: Nonlinear least squares, variable projection, weighted least squares, parameter estimation, SI engine.

## 1. INTRODUCTION

A newly developed engine, which can continuously change the compression ratio between 8.1 and 14.7 by tilting the mono-head, has been developed at SAAB Automobile AB. This ability to change the compression ratio opens up new opportunities to increase the efficiency of spark ignited (SI) engines by down sizing and super charging. But if the compression ratio gets stuck at too high ratios, the risk of engine destruction by heavy knock increases rapidly. If the compression ratio gets stuck at too low ratios, we get an unnecessary low efficiency, and therefore an unnecessary high fuel consumption. It is therefore vital to monitor and diagnose the continuously changing compression ratio. Due to geometrical uncertainties, a spread of the compression ratio among the different cylinders is inherent (Amann, 1985), and since it is hard to measure the compression ratio directly, estimation is required. The questions asked here are related to: 1) accuracy, 2) convergence speed and 3) over all convergence. The

approach investigated is to use cylinder pressure to estimate the compression ratio. A desirable property of the estimator is that it must be able to cope with the unknown offset introduced by the charge amplifier, changing thermodynamic conditions, and possibly also the unknown phasing of the pressure trace in relation to the crank angle revolution.

Two models for the cylinder pressure with different complexity levels, a polytropic model and a single-zone zero-dimensional heat release model (Gatowski et al., 1984) are used. To estimate the parameters in the cylinder pressure models, three different optimization algorithms minimizing the prediction error are utilized:

- (1) *A linear subproblem approach*, where groups of the parameters are estimated one at a time and the predictor function is rewritten to be linear for the group of estimated parameters. Thus linear regression can be used at every step for estimating the particular group of parameters.

- (2) A *variable projection method* (Björck, 1996), where one iteration consists of two steps: The first step estimates the parameters that are linear in the predictor function, holding the nonlinear constant. The second step is to perform a line search in the direction of the negative gradient at the parameters found from step one. This method classifies as a separable least squares method.
- (3) *Levenberg-Marquardt method*, i.e. a Gauss-Newton method with regularization, where numerical approximations of the gradient and the Hessian are used here.

Based on these models and optimization algorithms, four different compression ratio estimation methods applicable for both motored and fired cycles are given. It is explicitly stated how to use the methods for firing cycles as well as for motored, but the methods are only evaluated for motored cycles. The major step forward in this paper compared to Klein et al. (2004) is the evaluation on experimental data.

## 2. CYLINDER PRESSURE MODELING

Two models are used for describing the cylinder pressure trace and they are referred to as the polytropic model and the standard model.

**Polytropic model** A simple and efficient model is the polytropic compression model,

$$p(\theta)V(\theta)^n = C \quad (1)$$

where  $p(\theta)$  is the cylinder pressure,  $V(\theta)$  is the volume function,  $n$  is the polytropic exponent and  $C$  is a cycle-to-cycle dependent constant. The model describes the compression and expansion phase of the engine cycle well, but not the combustion phase (Heywood, 1988). Therefore, for a firing cycle only data between inlet valve closing (IVC) and start of combustion (SOC) will be used, but for motored cycles all data during the closed part of the cycle, i.e. between IVC and exhaust valve opening (EVO), is utilized.

**Standard model** Gatowski et al. (1984) develops, tests and applies the heat release analysis procedure used here. It maintains simplicity while still including the effects of heat transfer and crevice flows. The model has been widely used and the phenomena that it takes into account are well known (Heywood, 1988).

The pressure differential  $dp$  can be written as

$$dp = \frac{\delta Q_{ch} - \frac{\gamma}{\gamma-1} p dV - \delta Q_{ht}}{\frac{1}{\gamma-1} V + \frac{V_{cr}}{T_w} \left( \frac{T}{\gamma-1} - \frac{1}{b} \ln \left( \frac{\gamma-1}{\gamma'-1} \right) + T' \right)} \quad (2)$$

This ordinary differential equation is valid between IVC and EVO and can easily be solved numerically if a heat-release trace  $\delta Q_{ch}$  is provided, e.g. modeled by the Vibe function.

**Cylinder pressure referencing** Piezoelectric pressure transducers are used for measuring the in-cylinder pressure, which will cause a drift in the pressure trace, i.e. the absolute level is unknown and it is slowly varying. This drift is so slow that it is considered to be

constant during one engine cycle. The offset can be estimated with various methods (Randolph, 1990). Here the offset in the measured cylinder pressure  $p_m(\theta)$  is determined by comparing it to the intake manifold pressure  $p_{im}$  just before inlet valve closing (IVC), for several samples of  $p_{im}$ . Due to standing waves in the intake runners and flow losses over the valves at certain operating points, the referencing might prove to be insufficient. This is investigated by including a parameter for cylinder pressure bias in estimation methods 3 and 4, described in the next section.

## 3. ESTIMATION METHODS

Four methods are developed and investigated for compression ratio estimation. These methods are described below and their relations are summarized at the end of this section. All four methods are formulated as least-squares problems in a set of unknown parameters  $x$

$$\min_x \|\varepsilon(x)\|_2^2 \quad (3)$$

where a residual  $\varepsilon(x)$  is formed as the difference between a model and measurement. The differences between the methods lie in how the residuals are formed, and in the iterative methods used for solving the resulting problem (3).

The *termination criterion* for all methods are the same; If the relative improvement in the residual  $\|\varepsilon(x)\|_2$  is less than  $1 \cdot 10^{-6}$  in an iteration, the method terminates.

### 3.1 Method 1 – Sublinear approach

The first method uses the polytropic model (1)

$$p(\theta) (V_d(\theta) + V_c)^n = C \quad (4)$$

to estimate the polytropic exponent  $n$ , the compression ratio  $r_c$  and the constant  $C$ . The method iteratively solves two problems, one to determine the polytropic exponent  $n$ , and the other to determine the clearance volume  $V_c$  (i.e.  $r_c = (\max[V_d(\theta)] + V_c) / V_c$ ).

Applying logarithms on (4) yields the residual

$$\varepsilon_{1a}(C_1, n) = \ln p(\theta) - (C_1 - n \ln(V_d(\theta) + V_c)) \quad (5)$$

which is linear in the parameters  $C_1 = \ln C$  and  $n$ , if  $V_c$  is fixed. Another residual, that can be derived from (4), is

$$\varepsilon_{1b}(C_2, V_c) = V_d(\theta) - (C_2 p(\theta)^{-1/n} - V_c) \quad (6)$$

which is linear in the parameters  $C_2 = C^{1/n}$  and  $V_c$ , if  $n$  is fixed. The basic idea is to use the two residuals,  $\varepsilon_{1a}$  and  $\varepsilon_{1b}$ , iteratively to estimate the parameters  $n$ ,  $V_c$  and  $C$  by solving two linear least-squares problems. Using a Taylor expansion, see Klein (2004, pp.141), the following approximate relation between the residuals is obtained

$$\varepsilon_{1a}(\theta, x) \approx \frac{n}{V_d(\theta) + V_c} \varepsilon_{1b}(\theta, x) \quad (7)$$

The relation (7) must be taken into account and the residual  $\varepsilon_{1a}$  is therefore multiplied by the weight

$w(\theta) = V_d(\theta) + V_c$ , to obtain comparable norms in the least-squares problem. To use the weight  $w(\theta)$  is of crucial importance, and without it the algorithm diverges (Klein, 2004, pp.85). Convergence of the method can however not be proved. If the residuals were equal, i.e.  $\varepsilon_{1a} = \varepsilon_{1b}$ , the problem would be bilinear and the convergence linear (Björck, 1996). Each iteration in the algorithm is performed in three steps:

**Step 0:** Initialize the parameters  $x = [V_c \ C \ n]$ .

**Step 1:** Solve the weighted linear least-squares problem

$$\min_{n, C_1} \|w \cdot \varepsilon_{1a}\|_2^2$$

with  $V_c$  from the previous iteration.

**Step 2:** Solve the linear least-squares problem

$$\min_{V_c, C_2} \|\varepsilon_{1b}\|_2^2$$

with  $n$  from step 1.

**Step 3:** Check the termination criterion, if not fulfilled return to step 1.

### 3.2 Method 2 – Variable projection

The second method also uses the polytropic model (1), together with a variable projection algorithm. A nonlinear least-squares problem  $\min_x \|\varepsilon(x)\|_2^2$  is *separable* if the parameter vector can be partitioned  $x = (y \ z)$  such that

$$\min_y \|\varepsilon(y, z)\|_2^2 \quad (8)$$

is easy to solve. If  $\varepsilon(y, z)$  is linear in  $y$ ,  $\varepsilon(y, z)$  can be rewritten as

$$\varepsilon(y, z) = F(z)y - g(z) \quad (9)$$

For a given  $z$ , this is minimized by

$$y(z) = [F^T(z)F(z)]^{-1}F^T(z)g(z) = F^\dagger(z)g(z) \quad (10)$$

i.e. by using linear least-squares, where  $F^\dagger(z)$  is the pseudo-inverse of  $F(z)$ . The original problem  $\min_x \|\varepsilon(x)\|_2^2$  can then be rewritten as

$$\min_z \|\varepsilon(y, z)\|_2^2 = \min_z \|g(z) - F(z)y(z)\|_2^2 \quad (11)$$

and

$$\begin{aligned} \varepsilon(y, z) &= g(z) - F(z)y(z) = g(z) - F(z)F^\dagger(z)g(z) \\ &= (I - P_{F(z)})g(z) \end{aligned} \quad (12)$$

where  $P_{F(z)}$  is the orthogonal *projection* onto the range of  $F(z)$ , thus the name variable projection method.

Rewriting the polytropic model (1) as

$$\varepsilon_2(C_1, n, V_c) = \ln p(\theta) - (C_1 - n \ln(V_d(\theta) + V_c)) \quad (13)$$

results in an equation that is linear in the parameters  $C_1 = \ln C$  and  $n$ , and nonlinear in  $V_c$ . It is thus expressed on the form given in (9). A computationally efficient algorithm for compression ratio estimation, based on Björck (1996, p.352), is summarized in appendix A.

### 3.3 Method 3 – Levenberg-Marquardt and polytropic model

The third method uses the polytropic model (1), as methods 1 and 2 did, with an additive pressure sensor model added according to

$$p_m(\theta) = p(\theta) + \Delta p \quad (14)$$

in order to make the pressure referencing better. The pressure offset  $\Delta p$  is constant during one cycle. Furthermore, errors in the crank angle phasing  $\Delta\theta$  between the volume and pressure are also included in the polytropic model, which gives the following residual

$$\varepsilon_3(V_c, n, C, \Delta p, \Delta\theta) = p_m(\theta) - \Delta p - C \cdot (V_d(\theta + \Delta\theta) + V_c)^{-n} \quad (15)$$

A Levenberg–Marquardt method (Gill et al., 1981) is used to solve this nonlinear least-squares problem.

### 3.4 Method 4 – Levenberg-Marquardt and standard model

The fourth method uses the single-zone model (2) from Gatowski et al. (1984) which, in contrast to the other methods, also includes heat transfer and crevice effects. The model parameters used are given in (Klein, 2004, p.44). Due to the complexity of this model, the sublinear approach and variable projection approach are not applicable, and therefore only the Levenberg–Marquardt method is used. The increased complexity also causes identifiability problems for some of the parameters, since there exist many dependencies in between them. This is the case for the crevice volume  $V_{cr}$  and the clearance volume  $V_c$ , in which estimating the two parameters at the same time results in coupled and biased estimates. Therefore one of them is set constant, in this case the crevice volume (Klein, 2004, pp.94).

### 3.5 Summary of methods

Table 1 shows the relations between the methods. For firing cycles, methods 1, 2 and 3 use cylinder pressure data between IVC and SOC only, in contrast to method 4 which uses data from the entire closed part of the engine cycle. For motoring cycles, all data during the closed part of the cycle is utilized by all methods. It is also noteworthy that if the clearance volume  $V_c$  is considered to be known, methods 1 and 2 can be reformulated to instead estimate an additive pressure bias. Details are given in Klein (2004, pp.143).

Table 1. Relation between methods.

Alg./Model	Polytropic $p$	Standard $p$
Sublinear	Method 1	
Variable projection	Method 2	
Levenberg-Marquardt	Method 3	Method 4

## 4. SIMULATION RESULTS

Since the true values of the compression ratios of the engine are unknown, simulations of the cylinder pressure trace are necessary to perform and use for evaluating the four proposed methods. Cylinder pressure simulations were made using the standard model (2) with representative single-zone parameters, for integer compression ratios between 8 and 15. The results of these simulations were published in Klein et al. (2004) and are therefore only briefly recapitulated here.

*Estimation results* Figure 1 shows a summary of all estimates and table 2 displays e.g. the mean relative estimation error and the mean computational time. The estimations were made using Matlab 6.1 on a SunBlade 100, which has a 64-bit 500 Mhz processor.

Table 2. Relative mean error and 95 % relative confidence interval (RCI) in estimated  $r_c$  for all compression ratios. The mean computational time and number of iterations in completing one cycle are given.

M	$RE_{mean}$ [%]	RCI [%]	$RE_{max}$ [%]	std [-]	Time [ms]	#Iter [-]
1	0.9	4.4	1.3	0.038	52	5.8
2	-1.0	2.9	-1.1	0.034	18	3.0
3	-3.6	5.2	-4.3	0.110	73	3.9
4	0.2	0.3	0.3	0.002	$2 \cdot 10^5$	9.0

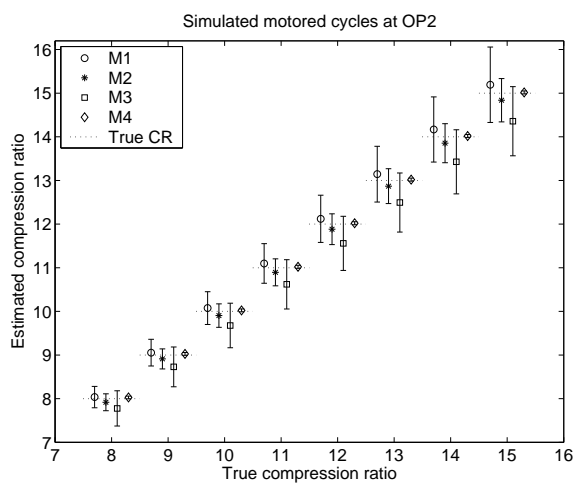


Fig. 1. Mean and 95% confidence interval of the estimated compression ratio for motored cycles using the four methods, compared to the true compression ratio. The estimate should be as close as possible to the dotted horizontal line.

*Analysis of estimation results* The first three methods rely upon the assumption of a polytropic compression and expansion. It is shown that this is sufficient to get a rough estimate of the compression ratio for motored cycles, especially for a low  $r_c$  and by letting the polytropic exponent become small. For a high  $r_c$  it is important to take the heat transfer into account, and then only method 4 is accurate within 0.5 % for all operating points. Method 4 is however slow and

not suitable for on-line implementation. Method 2 on the other hand is substantially faster and still yields estimates that are within 1.5 %. Using motored cycles assures that all pressure information available is utilized, and thereby decreases the confidence intervals.

A sensitivity analysis, with respect to crank angle phasing, cylinder pressure bias, crevice volume and heat transfer, shows that the third and fourth method are more robust. They therefore deal with these parameter deviations better than methods 1 and 2. Of the two latter, method 2 has the best performance for all parameter deviations except for an additive pressure bias.

## 5. EXPERIMENTAL RESULTS

The attention is now turned to the issue of evaluating the methods on experimental engine data. As mentioned before, the true value of the compression ratio is unknown. Therefore it is important to see if the effects and trends from the simulation evaluation are also present when the methods are applied to experimental data. The performance of the methods is discussed using one specific operating point, and is then followed by an evaluation including all operating points.

### 5.1 Experimental engine data

Data is collected during stationary operation at engine speeds  $N \in \{1500, 3000\}$  rpm, intake manifold pressures  $p_{im} \in \{0.5, 1.0\}$  bar altogether forming four different operating points, defined in table 4. The measurements are performed for actuated compression ratio values from the lower limit 8.13 to the upper limit 14.66, through integer values 9 to 14 in between. With actuated compression ratio it is meant the value commanded from the electronic control unit (ECU). These values were determined from engine production drawings and implemented in the ECU, but can be affected by production tolerances or non-ideal sensors (Amann, 1985), as well as mechanical and thermal deformation during engine operation (Lancaster et al., 1975).

For each operating point and compression ratio, 250 consecutive motored cycles with the fuel injection shut-off were sampled with a crank-angle resolution of 1 degree, using a Kiestler 6052 cylinder pressure sensor. Figure 2 displays one measured cycle for each  $r_c$  at operating point 2 (OP2). For a given  $r_c$  the monohead of the engine is tilted, which advances the position of TDC from 0 CAD for lowered compression ratios (Klein et al., 2003).

### 5.2 Results and evaluation for OP2

The performance of the estimation methods is first evaluated for OP2, defined in table 4. This operating

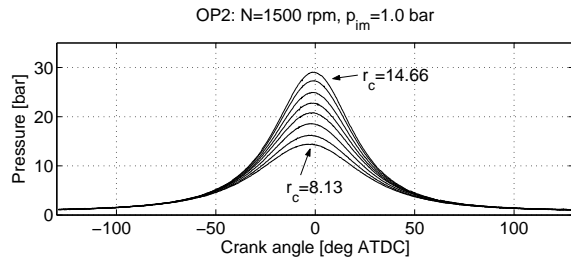


Fig. 2. Experimentally measured cylinder pressures at OP2. The actuated compression ratios are 8.13, integer values 9 to 14, and 14.66.

point has an intake manifold pressure in the midrange of the engine, and a relatively low engine speed for which the effects of heat transfer and crevices are significant. OP2 is therefore chosen as a representable operating point.

**Estimation results** The estimation results are presented in the same manner as for the simulated data. Figure 3 displays the mean estimate and the mean 95 % confidence interval for 250 consecutive cycles at OP2, where the estimate has been computed for each individual cycle. Table 3 shows mean computational time and mean number of iterations, as well as the relative mean error and 95 % relative confidence interval.

Table 3. Relative mean error, mean computational time and iterations, and mean 95 % relative confidence interval (RCI) at OP2.

M	$RE_{mean}$ [%]	RCI [%]	$RE_{max}$ [%]	std [-]	Time [ms]	#Iter [-]
1	6.4	5.3	8.1	0.11	89	6.8
2	3.6	3.8	5.1	0.083	19	2.7
3	-4.2	6.5	-6.1	0.066	114	4.1
4	2.1	1.3	3.5	0.048	$2 \cdot 10^5$	14.0

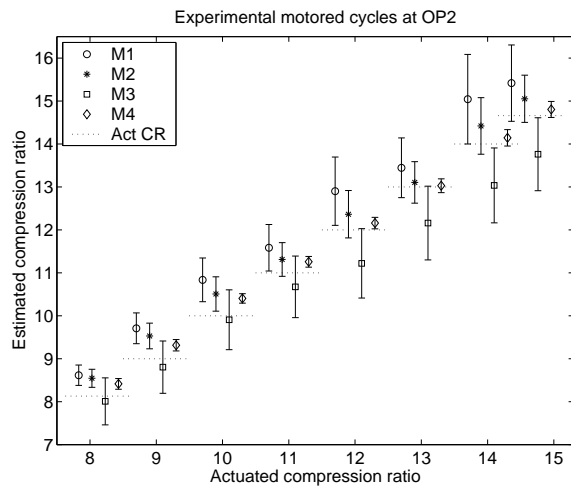


Fig. 3. Mean value and 95 % confidence interval of the estimated compression ratio for motored cycles using the four methods, compared to the actuated compression ratio. The estimate should be as close as possible to the dotted horizontal line.

**Analysis of estimation results** Figure 3 shows that method 3 underestimates and methods 1, 2 and 4 overestimate the compression ratio. The spread of the estimates between the methods is more pronounced than for the simulated data, compare figures 3 and 1. This spread increases as the compression ratio becomes higher, a trend also found for the confidence intervals of the estimates. The interrelation among methods 1-3 are however the same, where method 1 in average yields the largest estimates, and method 3 the smallest. The trends and effects in the simulation evaluation are also present in the experimental investigation, which gives a first indication that the conclusions drawn from the simulation study are valid.

All methods have larger confidence intervals for the experimental data, than for the simulated. This is due to the higher measurement noise level. Again method 4 yields the smallest confidence intervals followed by method 2. The difference is most significant for method 4, which had the correct model structure in the simulation case while here it is an approximation of the real engine. This is also seen in the residual, figure 4, as a systematic deviation around TDC. This model error thus adds to the variance of the estimate. It also changes the interrelation between methods 1-3 and method 4, e.g. method 4 gives in average a smaller estimate on experimental data than method 2, while the converse is valid for the simulated data.

The mean computational time and number of iterations are higher for the experimental data, as shown in table 3, which is probably due to a higher measurement noise level. As for the simulations, method 2 is the most computationally efficient method of them all.

**Residual analysis** The residuals corresponding to the cylinder pressures in figure 2 are displayed for all four methods in figure 4 for  $r_c = 14.66$ , together with their respective root mean square error (RMSE).

As for the simulations, see (Klein et al., 2004), there is a systematic deviation for methods 1, 2 and 3, which increases with  $r_c$ . The residual for method 4 have a

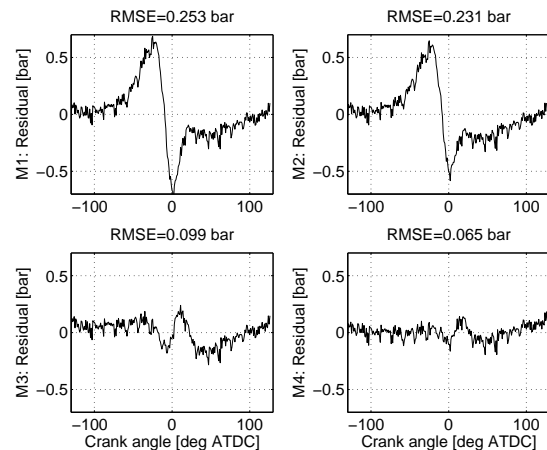


Fig. 4. Difference between estimated and experimental cylinder pressure for all methods, given the motored cycle in figure 2 at  $r_c = 14.66$ .

comparatively small deviation near TDC. This small deviation illustrates that the model structure is acceptable but not perfect, since it is not able to fully describe the measurement data. The relative mean error for  $r_c = 14.66$  is however small, less than 0.8 %, and method 4 can therefore be considered to capture the data well. The residuals from the experimental data have a higher RMSE compared to the simulations, but they are still of the same order. The differences between the methods are due to different formulations of the residuals and model simplifications. These properties give rise to the systematic deviations that are visible in both simulated and experimental data.

### 5.3 Results and evaluation for all OP

The trends shown for OP2 are also present in the full data set, displayed in table 4. This table shows that the influence of engine speed has no clear trend as two of the methods yield higher variance and the other two lower variance, as the engine speed is increased. However as the load increases, the variance for all methods decreases since the signal-to-noise ratio is improved while the effects of model errors in heat transfer and crevice flows remain the same. A high initial pressure is therefore desirable. For all operating points, method 4 yields the smallest confidence intervals followed by method 2.

Table 4. Relative mean error (RE) and mean 95 % relative confidence interval (RCI) in estimated  $r_c$ , for four operating points defined by engine speed  $N$  and intake manifold pressure  $p_{im}$ .

	OP1		OP2		OP3		OP4	
$N$	1500 rpm		1500 rpm		3000 rpm		3000 rpm	
$p_{im}$	0.5 bar		1.0 bar		0.5 bar		1.0 bar	
M	RE	RCI	RE	RCI	RE	RCI	RE	RCI
	[%]	[%]	[%]	[%]	[%]	[%]	[%]	[%]
1	10	6.2	6.4	5.3	8.0	7.5	3.6	5.9
2	6.0	4.6	3.6	3.8	1.3	5.2	-0.1	4.0
3	-2.3	8.2	-4.2	6.5	-3.9	7.3	-6.2	5.9
4	2.5	1.9	2.1	1.3	2.6	1.5	2.4	1.2

## 6. CONCLUSIONS

Two methods are recommended; If estimation accuracy has the highest priority, and time is available, method 4 should be used. Method 4 yields the smallest confidence intervals of all investigated methods for both simulated and experimental data. In the simulation case where the true value of the compression ratio is known, method 4 gave estimates with smallest bias. If computational time is the most important property, method 2 is recommended. It is the most computationally efficient of all investigated methods, and yields the smallest confidence intervals out of methods 1-3.

In order to estimate the compression ratio as accurately as possible, motored cycles with as high initial pressure as possible should be used.

## ACKNOWLEDGEMENTS

This work was financially supported by the *Swedish Agency for Innovation Systems (VINNOVA)*.

## REFERENCES

- C.A. Amann. Cylinder pressure measurement and its use in engine research. 1985. SAE Paper 852067.
- Å. Björck. *Numerical Methods for Least Squares Problems*. Siam, 1996.
- J.A. Gatowski, E.N. Balles, K.M. Chun, F.E. Nelson, J.A. Ekchian, and J.B. Heywood. Heat release analysis of engine pressure data. 1984. SAE Paper 841359.
- P.E. Gill, W. Murray, and M.H. Wright. *Practical Optimization*. Academic Press, 1981.
- J. B. Heywood. *Internal Combustion Engine Fundamentals*. McGraw-Hill, 1988.
- M. Klein. A specific heat ratio model and compression ratio estimation. Licentiate thesis, Vehicular Systems, Linköping University, 2004. LiU-TEK-LIC-2004:33.
- M. Klein, L. Eriksson, and Y. Nilsson. Compression estimation from simulated and measured cylinder pressure. *SAE 2002 Transactions Journal of Engines*, 111(3), 2003. SAE Paper 2002-01-0843.
- M. Klein, L. Eriksson, and J. Åslund. Compression ratio estimation based on cylinder pressure data. 2004. In proceedings of IFAC symposium on Advances in Automotive Control, Salerno, Italy.
- D. R. Lancaster, R. B. Krieger, and J. H. Lienesch. Measurement and analysis of engine pressure data. 1975. SAE Technical Paper 750026.
- A.L. Randolph. Methods of processing cylinder-pressure transducer signals to maximize data accuracy. 1990. SAE Technical Paper 900170.

## Appendix A. VARIABLE PROJECTION

A computationally efficient algorithm for variable projection (Björck, 1996, p.352) is summarized here. Partition the parameter vector  $x$  such that  $x = (y \ z)^T$ , where  $\varepsilon(y, z)$  is linear in  $y$ . Rewrite  $\varepsilon(y, z)$  as

$$\varepsilon(y, z) = F(z)y - g(z) \quad (\text{A.1})$$

Let  $x_k = (y_k, z_k)$  be the current approximation.

- (1) Solve the linear subproblem

$$\min_{\delta y_k} \|F(z_k)\delta y_k - (g(z_k) - F(z_k)y_k)\|_2^2 \quad (\text{A.2})$$

and set  $x_{k+1/2} = (y_k + \delta y_k, z_k)$ .

- (2) Compute the Gauss-Newton direction  $p_k$  at  $x_{k+1/2}$ , i.e. solve

$$\min_{p_k} \|C(x_{k+1/2})p_k + \varepsilon(y_{k+1/2}, z_k)\|_2^2 \quad (\text{A.3})$$

where  $C(x_{k+1/2}) = (F(z_k), \frac{\partial}{\partial z}\varepsilon(y_{k+1/2}, z_k))$  is the Jacobian matrix.

- (3) Set  $x_{k+1} = x_{k+1/2} + \alpha_k p_k$ , check the termination criterion and return to step 1 if the estimate has not converged. Otherwise return  $x_{k+1}$ .